International Journal of Innovative Research in Engineering and Management (IJIREM)
ISSN (Online): 2350-0557, Volume-11, Issue-3, June 2024
https://doi.org/10.55524/ijirem.2024.11.3.15
Article ID IJIR2557, Pages 92-98
www.ijirem.org

Numerical Examination of Loading Types Impact on Mat Foundations: A Case Study of a 10-storey Building in Gaziantep, Türkiye

M.Can Tekin[1], and Dr. Ayse Yeter Gunal[2]

[1] MSc. Scholar, Department of Civil Engineering, Faculty of Engineering, Gaziantep University, Gaziantep, Turkey
[2] Assistant Professor, Department of Civil Engineering, Faculty of Engineering, Gaziantep University, Gaziantep, Turkey

Correspondence should be addressed to M.Can Tekin; m.can.tekin1@gmail.com

Received: 24 May 2024 Revised: 7 June 2024 Accepted: 21 June 2024

ABSTRACT- This study leverages advanced numerical analysis techniques to model the intricate interactions among soil, foundation, and structures alongside the nonlinear load-deformation characteristics of soils in three-dimensional environments. This research underscores mat foundation calculations' enhanced realism and cost-efficiency, offering improvements over traditional methodologies. The objective is to explore the effects of different superstructure loading types on mat foundation behaviour using three-dimensional finite element models. Thirty-six distinct models were developed to examine the influence of superstructure loads, which were varied across uniformly distributed loads, column loads, and comprehensive building models. Each mat foundation was analysed using separate models incorporating 3D volume elements, utilizing the Mohr-Coulomb material model to represent soil conditions as either 'normally loaded' or 'over-consolidated.' The study presents detailed findings on total and differential settlements and internal forces, illustrated through figures and graphs, based on data from an existing ten-story building. Regarding bending moments, the most notable difference among loading types lies in the varied locations of maximum moments, independent of shear wall placement, particularly evident when simulating uniformly distributed loads. It is evident that the type of superstructure loading influences settlement patterns and internal forces, underscoring the necessity of considering this factor in analyses. Our findings reveal a significant disparity in construction costs between buildings erected on different soil classes, particularly between ZA and ZB. Structures situated on ZB-classified soil incur expenses approximately 1.5% higher than those on ZA-classified soil.

KEYWORDS- Mat foundation, Superstructure, Loading types, Soil Characterizations

I. INTRODUCTION

The soil characteristics, including strength, deformation, and other engineering properties, are inherently variable. Consequently, stress analyses within soil masses are notably more intricate than other civil engineering structures. This complexity intensifies when considering the collective interaction between soil, foundation, and superstructure. The mutual influence among the building, its foundation, and the underlying soils significantly impacts the behavior of each element and the overall system. The stresses and displacements of the structure and soil are affected by the relative stiffness of the building structure, its mat foundation, and the supporting soils.

Since soil typically exhibits lower strength than mat foundations, soil response is a crucial parameter in mat design. Ensuring compatibility between mat deflections and soil response is imperative for successful mat foundation design. However, soil-structure interaction effects are occasionally overlooked by employing a structural model supported on a fixed base or utilizing simplistic models that assume an ideally flexible or infinitely rigid foundation atop an elastic subsoil. Nevertheless, such oversimplified solutions have limited applicability due to the inherent complexity of the problems. Mat foundations encompass the entire structure and are designed to support the loads of multiple columns and/or shear walls. They are typically employed when the underlying soil has a low bearing capacity, or the column loads are significant enough to necessitate coverage exceeding about one-third or 50% of the area by conventional spread footings [1][2]. Mat foundations are widely favored in earthquake-prone regions due to their affordability and ease of waterproofing, owing to their monolithic structure [3]. Besides, an overview of the literature and current research on mat foundations has been created under a subheading

A. An Overview of Mat Foundations

While total settlements may pose challenges, the primary concern in mat foundation design is mitigating differential settlements. The tolerable levels of total or differential settlements depend on their potential impact on the superstructure and auxiliary facilities such as sewer, gas, or water lines. Employing methods that account for these tolerable settlements can lead to more economical designs. Recommended tolerable maximum settlements range from 64–102 mm for clays, 38–64 mm for sands, and tolerable differential settlements of 38 mm for clay and 25 mm for sand for rafts [4]. Flat-type mat foundations are favoured due to their straightforward construction process and their ability to generate unoccupied space. Despite being thicker

compared to other foundation types; they are recognized for providing superior economic benefits [5] [6].

Mat foundations alter the interaction between the structure and soil significantly compared to single and spread footings. Due to the complexity of soil-foundation-structure interaction, analysis and design require careful consideration and numerous assumptions based on soil reports [7]. Determining the base pressure distribution under mat foundations poses a challenge in calculating bending moments and shear forces. Over time, non-rigid analysis methods have become more prevalent alongside the advancement of numerical analysis methods, replacing the previously dominant use of rigid methods.

In rigid methods, the assumption that the plate is significantly stiffer than the underlying soils implies that any deformations in the mat will have negligible effects on the bearing pressures. Consequently, the bearing pressure distribution is solely determined by the building loads and the weight of the foundation. This distribution may either be uniform across the bottom of the mat or vary linearly depending on the location of the applied load [8]. However, the assumption of rigidity becomes invalid due to the relatively large width-to-thickness ratio of mats compared to other shallow foundations. Portions of the mat beneath columns and shear walls settle more than those with lighter loads, resulting in higher bearing pressures beneath heavily loaded areas. This perspective fails to account for the actual distribution of base pressures, potentially leading to inaccuracies in calculated moments, shears, and deflections. Nevertheless, rigid methods remain popular due to their suitability for hand calculations [4] [9].

Instead, non-rigid methods consider the distribution of bearing pressures and their impact on deflections without assuming complete rigidity of the mat foundation. While their results are generally more reliable than those of rigid methods, they pose challenges in calculations because predicting soil-structure interaction is not as straightforward. Early studies in this area, pioneered by Terzaghi et al. [10], employed the Winkler hypothesis to model the soil as independent elastic springs. Through this approach, efforts were made to define the relationship between bearing pressures and settlements [11].

This approach conceptualizes the interaction between the mat foundation and the soil as a "bed of springs" [12]. While this method offers significant improvements over rigid methods, such as increased bearing pressure under columns, it was later recognized that there were inconsistencies in this approach. As a result, the relationship between the springs was incorporated into the model to provide a more refined solution [13-17]. Although the springs can operate independently using the latest alternative methods, the spring stiffness (ks) value varies based on its location along the mat. Achieving the desired dish-shaped deformation in a uniformly loaded mat involves approximately twofold stiffening of the outermost zone springs. It has been recommended that the "rigid method" be utilized solely for preliminary design and the "dishing phenomena" be considered not only for predicting mat settlements but also in the structural design of the mat foundations [18].

Today, in software packages (such as SAP2000, SAFE, PcaMats, STA4CAD, etc.) commonly used by civil engineers, soil spring coefficients are calculated using subgrade reaction modules. Elastic soil beneath the plate is represented by soil springs specified at the nodes of plate elements. These soil springs can be calculated by multiplying each node's effective area and subgrade reaction modules. The effective area for each node is the sum of the areas of each neighbouring element [19]. However, it's important to note that modeling a 3D soil problem with a series of one-dimensional springs is acceptable only for simplifying the problem to conduct structural analysis. Whereas Sert and Kılıç [20] argued that obtaining an exact solution by considering all soil and superstructure properties is impossible, simplified calculations are commonly used to solve the problem. In contrast to this view, advancements in computer technology and numerical analysis methods have popularized numerical analysis in geotechnical engineering problems, including soil-structure interactions. In numerical analysis, the problem can be modeled in 3D, allowing for investigating the effects of neighbouring buildings simultaneously with settlement and deflections. Furthermore, using numerical analysis has been shown to lead to more economical designs than conventional methods [21] [22].

II. METHODOLOGY AND DATASET

A. Choosing the Appropriate Earthquake Ground Motion for Analytical Purposes

Following the devastating earthquakes in Gölcük and Bolu in 1999, the Ministry of Public Works and Settlement released the Seismic Zoning Map of Turkey in 2000, using probability methods whereby Table 1 displays the distribution of seismic hazard risk across Turkey. According to the findings, 66% of Turkey's land area falls within the 1st and 2nd-degree earthquake zones, essentially active fault zones (zones characterized by fractures along fault lines), whereas 74% of the population resides in these regions [23].

Table 1. Distributions of seismic hazards in Türkiye [23]

SEISMIC HAZARD ZONE	SURFACE AREA (%)	POPULATION (%)	INDUSTRY (%)	DAMS (%)
1st Degree Earthquake Zone	42	45	51	46
2nd Degree Earthquake Zone	24	26	25	23
3rd Degree Earthquake Zone	18	14	11	14
4th Degree Earthquake Zone	16	15	13	17
TOTAL	100	100	100	100

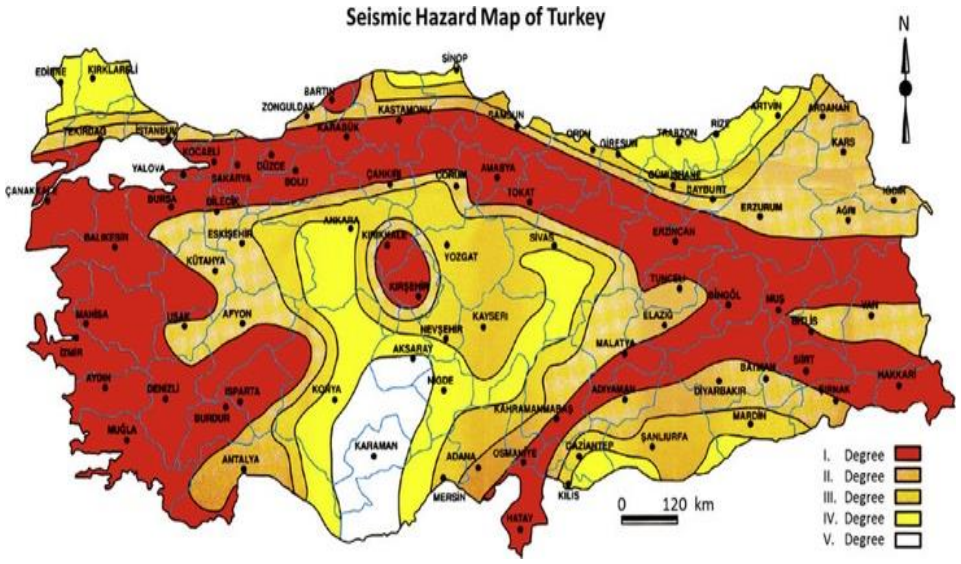

Figure 1. Seismic hazard map of Türkiye, according to TSDC 2018.

Examining Table 1, it is clear which seismic regions require detailed analysis and design to mitigate the effects of potential future earthquakes. Beyond tectonic movements, other critical factors like soil conditions significantly influence a structure's seismic response. These elements must be included in the seismic analysis and design processes for all types of buildings. According to the Turkish Seismic Code, four main soil groups (ZA, ZB, ZC, and ZD) are categorized based on subterranean geological conditions. These categories are further broken down into local site classes (Z1, Z2, Z3, and Z4), depending on the thickness of the topsoil layer. To forecast the seismic behavior of structures during intense ground motions, it is crucial to consider the local soil conditions at a site because they can either amplify or reduce the effects seen in the response spectrum [24]. Hong et al. [24] discuss soil amplification effects. The Building Research Institute (BRI) of the Ministry of Construction and the Association for Promotion of Building Research (APBR) in Sendai, Japan, began collecting earthquake data in 1983 after setting up seismic recording stations. The study covered a range of surface geological conditions, including rock outcrops, reclaimed lands, and soft soil areas.

Although the project's duration was too short to gather extensive data, researchers acquired various insights into soil amplification and the variations in subsurface earthquake motions. Under the Turkish Seismic Design Code (TSDC 2018), soil groups are classified into ZA, ZB, ZC, ZD, ZE, and ZF based on the design acceleration spectrum. The ZA soil group consists of solid, hard rock; less weathered, moderately solid rocks characterize ZB; ZC includes very dense sand, gravel, and hard clay layers; ZD comprises gravel or clay layers; ZE contains loose sand and soft clay; and ZF soil layers necessitate site-specific research and evaluation. The spectral acceleration coefficients for these groups are detailed in Table 2. Comparisons between the Turkish Earthquake Code 2007 (TEC) and TSDC 2018 reveal that the Z1 soil class exhibits characteristics similar to those of the ZA soil group.

B. Illustration Building Details for Modeling

The structure examined in this study consists of two blocks with a 10-storey building and 2-ground floors with a comprehensive floor space of 755 square meters for each block. Detailed architectural layouts, including the ground floor and elevation plans, are presented in Figures 2a and 2b, respectively. These technical drawings are essential for analyzing the spatial distribution and structural dimensions critical for scientific assessment and modeling.

This study involved the static analysis of structures tailored to various soil classes using Sta4-CAD [25] is the Turkish project market's leading structural analysis software. It was presumed that all the buildings are situated in the 1st-degree seismic zone, as illustrated in Figure 1 and designed by diverse local soil classes. According to the Turkish Seismic Design Code (TSDC, 2018), this seismic zone's effective ground acceleration coefficient was set at 0.40. This coefficient is crucial for ensuring the structural integrity and seismic safety of the buildings analyzed.

Table 2: Spectral acceleration coefficients, according to TSDC 2018

Soil Group	$S_1 \leq 0.1$	$S_1 = 0.2$	$S_1 = 0.3$	$S_1 = 0.4$	S1=0.5	S1≥0.6
ZA	0.8	0.8	0.8	0.8	0.8	0.8
ZB	0.8	0.8	0.8	0.8	0.8	0.8
ZC	1.5	1.5	1.5	1.5	1.5	1.4
ZD	2.4	2.2	2.0	1.9	1.8	1.7
ZE	4.2	3.3	2.8	2.4	2.2	2.0

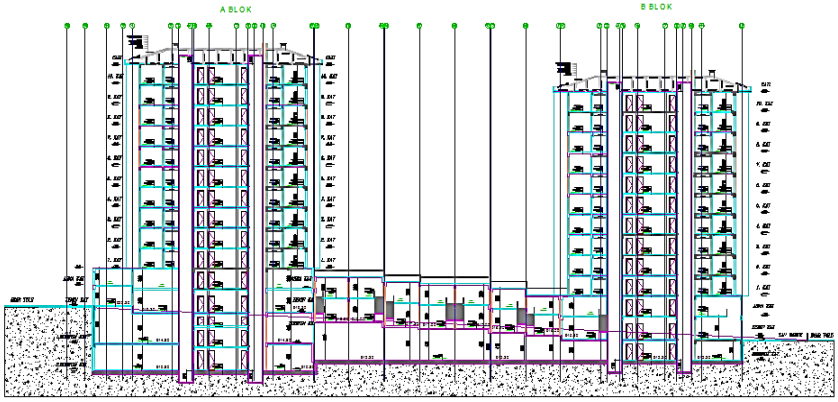

(a)

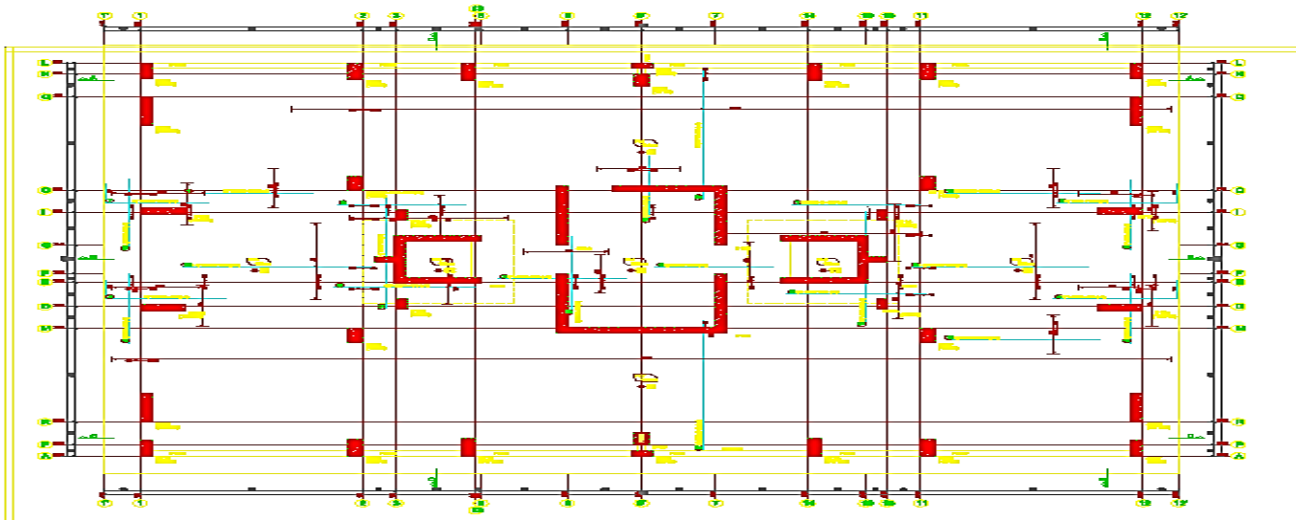

(b)

Figure 2(a) (b): Plan of the modeled two blocked buildings in the (a) & side view of building blocks and (b) foundation plan

III. RESULTS AND DISCUSSION

A. Characteristics of Simulated Building Conditions in Computational Models

This study utilized data from an existing building to create models (Figures. 2a and 2b). The building, designed with three stories of varying heights, sits atop a flat mat foundation with a thickness of 120 cm. Its dimensions are 16.80 m by 12.45 m, with symmetry along one axis. The structure comprises one shear wall and 21 columns of different sizes, with beams measuring 0.25 m by 0.5 m and slab thicknesses of 0.16 m, as given in Figure 2b.

Distinct models were developed to investigate the impact of loading types on internal forces and settlement behavior in different soil possessions. Mat and superstructure elements, including columns, slabs, and shear walls, were modeled using either 2D plate elements or 3D volume elements across different models. The term of "uniformly distributed load" refers to the equal distribution of building loads across the foundation. In this loading scenario, a load of ~34 kPa is applied uniformly by dividing the total load of 6800 kN by the foundation's footprint area. In the finite element method, increasing the number of elements in areas where stress concentration occurs leads to more accurate results [3, 4, 6]. The soil is modeled in 3D, with model dimensions set at 50 m by 120 m by 40 m. Determining these dimensions involved evaluating the volumes influenced by loading in the models and calculation times. Global and local refinements were implemented in areas where stress concentration was expected. Additionally, element sizes were increased in the corners and sides of the model to reduce computational time. The software allows for the representation of soil properties using the "Modified Mohr-Coulomb" model, which is adept at simulating the hyperbolic elastic-plastic behavior of various types of soils, ranging from soft to stiff. Alternatively, the simpler linear elastic-perfectly plastic "Mohr-Coulomb" model can be utilized (Figure 3).

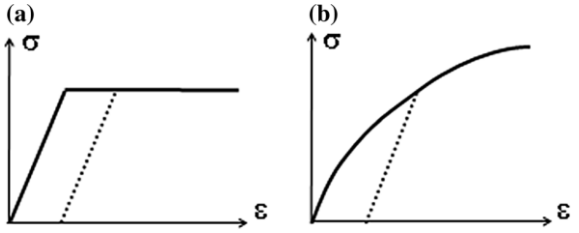

Figure 3(a) (b): Stress-strain behavior models for soils(a) Linear elastic–perfectly plastic, (b) nonlinear elastic–hardening plastic

In the elastoplastic Mohr-Coulomb model, parameters such as E (Young's modulus or deformation modulus), m (Poisson's ratio), c (cohesion), u (angle of shearing resistance), and w (dilatancy angle) characterize the elastic and plastic behavior as well as volume change. When investigating stress-strain behavior for soil and rock, employing a constant average rigidity for all layers based on the Mohr-Coulomb failure criteria aids in accelerating calculations and providing a rough estimate of potential displacements.

Once the model geometries were established, soil properties were defined and attributed. This study used the "Mohr-Coulomb" material model, and two hypothetical data sets were prepared to represent soil properties as "normally loaded" and "over-consolidated." Over-consolidated soils, characterized by an effective overburden pressure lower than past pressures, are anticipated to exhibit greater bearing capacity and reduced settlement under load. The ratio between past and present overburden stresses, known as the over-consolidation ratio (OCR), typically equals unity in normally consolidated soils but may exceed unity, such as values of two or five in over-consolidated soils. The models calculated the lateral earth pressure coefficient (K0), representing the ratio between horizontal and vertical stresses under conditions, using u for normally loaded soil and u and OCR for over-consolidated soil. The soil profile comprised a single layer with constant stiffness and resistance, while foundation and superstructure elements were attributed with reinforced concrete properties.

B. Findings of Static Examination and Assessments

This study employed static analyses of structures designed based on various soil classifications, utilizing Sta4-CAD, a prevalent structural analysis software within the Turkish project market. It was assumed that all buildings were situated in the first-degree seismic zone, as depicted in Figure 1, and were engineered in accordance with distinct local soil classifications. The effective ground acceleration coefficient was set at 0.40 for the first-degree earthquake zone, as stipulated by the Turkish Seismic Design Code (TSDC 2018). Our modeling approach has been limited to only ZA and ZB due to geological conditions in the Gaziantep region. Figure 4 showcases the soil tension around the foundation plate for different loading conditions using 3D element models in soil type A with a thickness of 50 cm. Notably, the tension values for uniformly distributed-loaded and building-loaded models are quite similar, ranging from 18.4 to 51.82 kPa, particularly evident in the column-loaded model. It is crucial to note that the location of maximum displacement shifts significantly depending on whether the load is distributed across the entire structure or focused at specific points. This variation influences the calculation of internal forces and suggests that adjustments in reinforcement placement might be necessary to accommodate the different stress distributions observed under various loading scenarios.

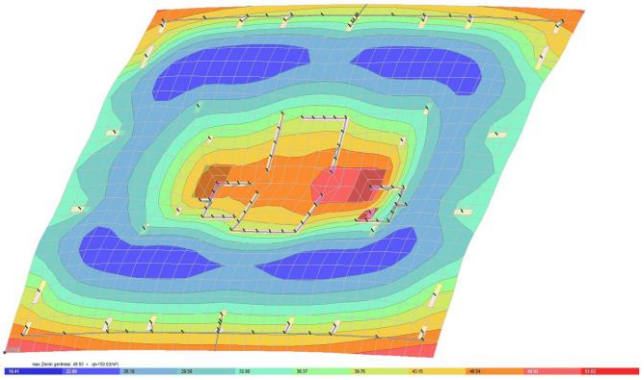

Figure 4: The deflection of the foundation plate in 3D element models with ZA soil conditions

Figure 5 reveals that total settlements tend to decrease in relation to the ZB class soil configurations, indicating a robust correlation between soil class and settlement reduction. Similarly, the differential settlements also show a declining trend as the foundation thickness increases, as observed across all calculations for both soil types, depicted in Figures 4 and 5. Conversely, for uniformly distributed loads, while the building-loaded model displays a pressure close to ZA class soil (ranging from 18.4 to 50.12 kPa), this pressure notably diminishes to approximately 1.5 kPa when applied solely to the foundation. This contrast underscores the significant influence of foundation characteristics on load distribution and soil pressure response.

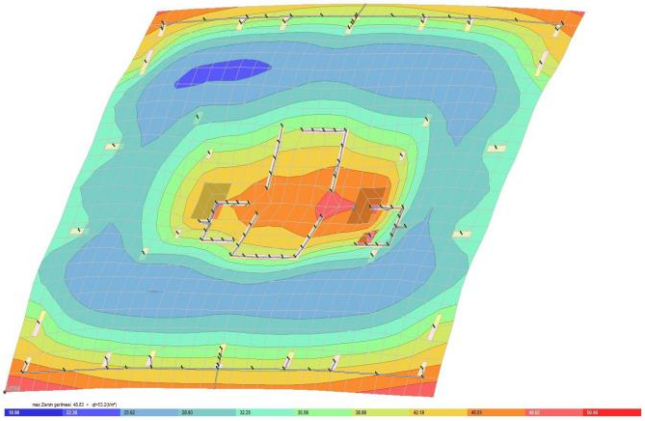

Figure 5: The deflection of the foundation plate in 3D element models with ZB soil conditions

The maximum values for total and differential displacements for all models are summarized in Table 3. As the thickness of the foundation increases, the maximum total displacements exhibit a decreasing trend for all types of loading in 3D element models. Conversely, in models using 2D elements, while total settlements increase, differential settlements seem to decrease for all types of loading. This discrepancy is attributed to the increasing rigidity with plate thickness in 3D element models. The absence of the embedment depth effect in 2D element models also contributes to increased vertical reimbursements.

Table 3 and figures 4 and figure 5 demonstrated that maximum bending moments are significantly higher when column-transmitted loads to the foundation. In soil ZA and

ZB, the maximum M_{xx} moment ratios between column-loaded and building-loaded models are 3.18 and 3.24, respectively. These differences are even more pronounced in M_{yy} values, reaching 3.19 and 4.17. In conditions of relatively soft soil, bending moments are typically higher than those in stronger soil. This variance is more pronounced in models loaded by columns and distributed loads. The differences in bending moments decrease as the thickness of the foundation increases. The fact that the amount of buckling caused.

Table 3: Bending and torsional moments for models ZA (up) and ZB (down)

Plak no	D cm	mesh x	mesh y	Ko t/m³	g t/m²	p t/m²	X1	Y1	Z1	X2	Y2	Z2
PL1	120	30	11	15000	3.000	0.000	-1.00	-1.00	0.00	29.40	-1.00	0.00
PL2	120	8	2	15000	3.000	0.000	-1.00	10.20	0.00	7.50	10.20	0.00
PL7	120	30	11	15000	3.000	0.000	-1.00	12.55	0.00	29.40	12.55	0.00
PL6	120	9	2	15000	3.000	0.000	20.30	10.20	0.00	29.40	10.20	0.00
PL4	120	9	2	15000	3.000	0.000	9.40	10.20	0.00	18.40	10.20	0.00
PL3	120	2	2	15000	3.000	0.000	7.50	10.20	-1.70	9.40	10.20	-1.70
PL5	120	2	2	15000	3.000	0.000	18.40	10.20	-1.70	20.30	10.20	-1.70
PL1	120	2	2		3.000	0.000	9.40	10.20	0.00	9.40	10.20	-1.70
PL2	120	2	2		3.000	0.000	20.30	10.20	0.00	20.30	10.20	-1.70
PL7	120	2	2		3.000	0.000	7.50	10.20	0.00	7.50	10.20	-1.70
PL6	120	2	2		3.000	0.000	7.50	12.55	0.00	7.50	12.55	-1.70
PL4	120	2	2		3.000	0.000	18.40	12.55	0.00	18.40	12.55	-1.70
PL3	120	2	2		3.000	0.000	20.30	12.55	0.00	20.30	12.55	-1.70
PL5	120	2	2		3.000	0.000	9.40	12.55	0.00	9.40	12.55	-1.70
	120	2	2		3.000	0.000	18.40	10.20	0.00	18.40	10.20	-1.70

Plak no	D cm	mesh x	mesh y	Ko t/m³	g t/m²	p t/m²	X1	Y1	Z1	X2	Y2	Z2
PL1	120	30	11	12000	3.000	0.000	-1.00	-1.00	0.00	29.40	-1.00	0.00
PL2	120	8	2	12000	3.000	0.000	-1.00	10.20	0.00	7.50	10.20	0.00
PL7	120	30	11	12000	3.000	0.000	-1.00	12.55	0.00	29.40	12.55	0.00
PL6	120	9	2	12000	3.000	0.000	20.30	10.20	0.00	29.40	10.20	0.00
PL4	120	9	2	12000	3.000	0.000	9.40	10.20	0.00	18.40	10.20	0.00
PL3	120	2	2	12000	3.000	0.000	7.50	10.20	-1.70	9.40	10.20	-1.70
PL5	120	2	2	12000	3.000	0.000	18.40	10.20	-1.70	20.30	10.20	-1.70
PL1	120	2	2		3.000	0.000	9.40	10.20	0.00	9.40	10.20	-1.70
PL2	120	2	2		3.000	0.000	20.30	10.20	0.00	20.30	10.20	-1.70
PL7	120	2	2		3.000	0.000	7.50	10.20	0.00	7.50	10.20	-1.70
PL6	120	2	2		3.000	0.000	7.50	12.55	0.00	7.50	12.55	-1.70
PL4	120	2	2		3.000	0.000	18.40	12.55	0.00	18.40	12.55	-1.70
PL3	120	2	2		3.000	0.000	20.30	12.55	0.00	20.30	12.55	-1.70
PL5	120	2	2		3.000	0.000	9.40	12.55	0.00	9.40	12.55	-1.70
	120	2	2		3.000	0.000	18.40	10.20	0.00	18.40	10.20	-1.70

The low effect of heavily loaded structural elements in ZA and ZB class soils, which have high geological differences between the units, shows that an optimization of the materials used in the building is also necessary. An example cost table for this optimization is given in Table 4.

Table 4: Calculating Quantities and Costs for Modelled Building in 2024, local field conditions

Model No.	Soil Class	(Ko) Soil Bearing Class. (t/m³)	(qt) Soil Bearing Stress (t/m²)	Iron quantity (kg)	Concrete quantity (m³)	Mold quantity (m²)	Steel Class	Concrete Class
1	ZB	12000.00	53.20	39859.5	928.44	189.56	S420B	C30
2	ZA	15000.00	150.00	39246.6	928.44	189.56	S420B	C30

Additionally, the most significant decreases in differential settlements occur in column and building loading as soil properties improve, whereas this effect remains minimal in distributed loading scenarios. The Ministry of Environment and Urbanization has set official unit costs for materials, considering potential price variations due to regional and brand differences. The analysis revealed a significant ~%1.56 cost difference, plus ~613 kg iron cost, in building buildings on local soil classes ZA and ZB. The order of the structural elements of the building foundation formed by both models and their physical parameters are given in detailed tables under the supplied materials heading.

IV. CONCLUSION

In this study, under the 2018 Turkish seismic building code, the impact of local soil conditions on the seismic responses of buildings and consequent changes in building costs were examined using a specific structure. Due to the incompatibility of the Sta4-Cad software used in the study with the newly developed soil parameters of the 2018 code, several assumptions were necessary. This incompatibility introduces a limitation in the analysis phase of the study.

Figures 4 and 5 summarize the stress distribution from foundations under various loading conditions. As indicated in Figures 4 and 5, the maximum bending moments and torsional moments tend to increase with increasing foundation thickness. The maximum bending moments are highest when loads are transmitted to the foundation via columns. The ratio of the maximum values of Mxx moments between column-loaded and building-loaded models appears to reach a maximum.

This study demonstrates numerically that the loading type of

the superstructure significantly influences both settlement patterns and internal forces. Using 3D elements resulted in lower total and differential displacements compared to models employing 2D elements. Furthermore, building-loaded models exhibited lower bending moments and differential settlements than other loading types. The analysis revealed distinct characteristics across different loading types: varying locations of maximum displacements, settlement patterns of the foundation, maximum and differential settlement values, and bending and torsional moment values. These differences highlight the interaction between the superstructure, foundation and soil. Although there is not a huge design difference, as observed in the model coefficients, this difference in the building materials used in the foundation (ZA 39.426 kg and ZB 39.589 kg) makes it possible to provide absolute resistance against the earthquake load on ZB conditional floors. For this reason, pre-manufacturing modeling constitutes an extremely necessary phase.

Employing the three-dimensional finite element method allows for consideration of the rigidities of the superstructure, the mat itself, and the underlying soil. As such, it currently stands as the most accurate model for analyzing soil-structure systems, offering economically viable solutions.

CONFLICTS OF INTEREST

The authors declare that they have no conflicts of interest.

ACKNOWLEDGMENT

Special thanks to the reviewers for their constructive feedback, which greatly enhanced the quality of this study. I am thankful for the support of my peers and family, who have been instrumental in this journey. I confirm that no external funding was used for the modeling in this study.

REFERENCES

1) D. P. Coduto, “Foundation design: principles and practices”. Pearson Education Limited, 2014.
2) M. Budhu, “Foundations and earth retaining structures”. 2008.
3) L. Pasticier, C. Amadio, and M. Fragiacomo, "Non-linear seismic analysis and vulnerability evaluation of a masonry building by means of the SAP2000 V. 10 code," Earthquake Eng. Struct. Dyn., vol. 37, no. 3, pp. 467-485, 2008.
4) J. E. Bowles and Y. Guo, “Foundation analysis and design”, vol. 5. New York: McGraw-Hill, 1996, p. 127.
5) R. L’Herminier, M. Bachelier, and F. Soeiro, "Investigation on the foundation raft for the first atomic reactor at Marcoule," in Proc. 4th Int. Conf. Soil Mech. Found. Eng., London, vol. 1, 1957, pp. 307–311.
6) J. Morrison, "Raft foundations for two Middle East tower blocks, design applications of raft foundations," in Design Applications of Raft Foundations, J. A. Hemsley, Ed. London: T. Telford, 2000, pp. 155–172.
7) E. J. Ulrich, "An introduction to the state-of-the-art mat foundation design and construction," in Design and Performance of Mat Foundations, E. J. Ulrich, Ed. USA: ACISP-152, 1995, pp. 1–12.
8) A. R. Gaba, B. Simpson, W. Powrie, and D. R. Beadman, “Embedded retaining walls: guidance for economic design”, RP 629. London: Construction Industry Information and Research Association, 2002.
9) J. S. Horvath and R. J. Colasanti, "Practical subgrade model for improved soil-structure interaction analysis: Model development," Int. J. Geomech., vol. 11, no. 1, pp. 59-64, 2011.
10) K. Terzaghi, R. B. Peck, and G. Mesri, “Soil mechanics in engineering practice”, John Wiley & Sons, 1996.
11) R. L. Hall, "Spring stiffness for beam-column analysis of soil-structure interaction problems," Ph.D. dissertation, Oklahoma State University, 1984.
12) N. K. Rao, “Foundation design: theory and practice”. John Wiley & Sons, 2010.
13) L. A. Wood, "The economic analysis of raft foundations," Int. J. Numer. Anal. Methods Geomech, vol. 1, no. 4, pp. 397-405, 1977.
14) A. D. Kerr, "On the determination of foundation model parameters," J. Geotech. Eng., vol. 111, no. 11, pp. 1334-1340, 1985.
15) M. Verman, B. Singh, J. L. Jethwa, and M. N. Viladkar, "Determination of support reaction curve for steel-supported tunnels," Tunnell. Undergr. Space Technol, vol. 10, no. 2, pp. 217-224, 1995.
16) J. F. Horvilleur and V. B. Patel, "Mat foundation design: a soil-structure interaction problem," Special Publication, vol. 152, pp. 51-94, 1995.
17) J. S. Horvath and R. J. Colasanti, "Practical subgrade model for improved soil-structure interaction analysis: Model development," J. Geotech. Eng., vol. 11, no. 1, pp. 59-64, 2011.
18) S. W. Tabsh and M. El-Emam, "Influence of foundation rigidity on the structural response of mat foundation," Adv. Civ. Eng., vol. 2021, pp. 1-13, 2021.
19) L. Pasticier, C. Amadio, and M. Fragiacomo, "Non-linear seismic analysis and vulnerability evaluation of a masonry building by means of the SAP2000 V. 10 code," Earthquake Eng. Struct. Dyn., vol. 37, no. 3, pp. 467-485, 2008.
20) S. Sert and A. N. Kılıç, "Numerical investigation of different superstructure loading type effects in mat foundations," Int. J. Civ. Eng., vol. 14, pp. 171-180, 2016.
21) O. Ravaska, "A sheet pile wall design according to Eurocode7 and Plaxis," Numerical Methods in Geotechnical Engineering, P. Mestat, Ed. Paris: Presses de l’ENPC/LCPC, 2002, pp. 649–654.
22) A. R. Gaba, B. Simpson, W. Powrie, and D. R. Beadman, “Embedded retaining walls: guidance for economic design”, RP 629. London: Construction Industry Information and Research Association, 2002.
23) G. Ertan, "Civil society and disaster management: case of Marmara Earthquake," Electron. Soc. Sci. J., vol. 19, no. 76, pp. 2044-2056, 2020.
24) J. Y. Hong, S. W. Ahmad, A. Adnan, K. Muthusamy, N. F. Ariffin, F. M. Yahaya, and S. M. S. Mohsin, "Seismic performance and cost analysis for reinforced concrete school building under different type of soil," Phys. Chem. Earth, Parts A/B/C, vol. 120, p. 102933, 2020.
25) STA4CAD, “Analysis and design manual of multi-storey RC structures”, V13.1. STA Computer Engineering and Consulting Company, Istanbul, Turkey, 2010.